

Article

Influence of Iron-Enriched Biochar on Cd Sorption, Its Ionic Concentration and Redox Regulation of Radish under Cadmium Toxicity

Fiza Pir Dad ¹, Waqas-ud-Din Khan ^{1,2,*} , Mohsin Tanveer ^{2,*} , Pia Muhammad Adnan Ramzani ³, Rabia Shaukat ¹ and Abdul Muktedir ⁴ 

¹ Sustainable Development Study Centre, Government College University, Lahore 54000, Pakistan; fizapirdad@yahoo.com (F.P.D.); rabia.shaukat@gmail.com (R.S.)

² Tasmanian Institute of Agriculture, University of Tasmania, Hobart 7005, Australia

³ Cholistan Institute of Desert Studies, The Islamia University of Bahawalpur, Bahawalpur 63100, Pakistan; dr.piamuhammad@iub.edu.pk

⁴ Pulses Research Centre, Bangladesh Agricultural Research Institute, Gazipur 1701, Bangladesh; muktadirgpb@gmail.com

* Correspondence: dr.waqasuddin@gcu.edu.pk (W.-u.-D.K.); mohsin.tanveer@utas.edu.au (M.T.)

Abstract: Cadmium (Cd), a potent heavy metal, causes a significant reduction in plant growth and its yield by interfering with the plant's mineral nutrition and, primarily, by inducing Cd-induced oxidative damage. Cd mobilization at the soil–root interface is also very important in context of its bioavailability to plants. Therefore, an experiment was carried out to evaluate the mitigating role of iron-enriched biochar (Fe-BC) on Cd accumulation in soil and Cd toxicity in radish plants. Radish seeds were sown in pots, and two levels of Cd (0 and 0.75 mg kg^{−1}) and two levels of Fe-BC (0 and 0.5%) were applied. Cd stress significantly reduced radish fresh and dry biomass production, which was due to high production of malondialdehyde (36%) and increase in cell membrane permeability (twofold) relative to control. Moreover, Cd stress considerably reduced chlorophyll concentrations and uptake of some essential nutrients, such as Ca, K, and Fe. Contrarily, Fe-BC application ameliorated Cd toxicity by triggering the activation of antioxidant enzymes (catalase and ascorbate peroxidase), primary and secondary metabolite accumulation (protein and phenolics concentrations), and by improving plant mineral nutrition under Cd treatment, compared with Cd treatment only. The ability of biosorbent material (Fe-BC) to adsorb the Cd ion on its surface and its immobilization from Cd-polluted soil to plant root was determined by using Langmuir and Freundlich isotherm models. Interestingly, Cd concentration was found in soil as diethylenetriamine (DTPA)-extractable soil Cd on radish root, but not reported in radish shoot with Cd+Fe-BC treatment, compared to Cd treatment; suggesting that Fe-BC treatment has a potential to provide extra strength to the root and shoot, and plays an important role in regulation ionic and redox homeostasis under Cd stress.

Keywords: antioxidants; biochar; cadmium toxicity; reactive oxygen species; Langmuir and Freundlich equations; nutrients uptake



Citation: Dad, F.P.; Khan, W.; Tanveer, M.; Ramzani, P.M.A.; Shaukat, R.; Muktedir, A. Influence of Iron-Enriched Biochar on Cd Sorption, Its Ionic Concentration and Redox Regulation of Radish under Cadmium Toxicity. *Agriculture* **2021**, *11*, 1. <https://doi.org/10.3390/agriculture11010001>

Received: 23 November 2020

Accepted: 18 December 2020

Published: 22 December 2020

Publisher's Note: MDPI stays neutral with regard to jurisdictional claims in published maps and institutional affiliations.



Copyright: © 2020 by the authors. Licensee MDPI, Basel, Switzerland. This article is an open access article distributed under the terms and conditions of the Creative Commons Attribution (CC BY) license (<https://creativecommons.org/licenses/by/4.0/>).

1. Introduction

Plants are an integral part of the ecosystem, contributing a significant portion to the food chain. Under the current climate change situation, both biotic stresses (e.g., pathogen and insect infestation) and abiotic stresses (e.g., soil salinity, waterlogging, drought, and high temperature) are the significant constraints for sustainable crop production [1–6]. Therefore, agriculture needs to be revolutionized at a rapid rate to maximize production and to meet the increasing demand for food with the booming population [7]. Cadmium (Cd) is one of the major environmental threats to agricultural systems due to its high residence

time (>1000 years) in soil [8]. As Cd has high mobility in soil and is hydrophilic in nature, it readily accumulates in plants and reduces plant growth and development [1,9]. Cd toxicity reduced plant growth and its yield by up to 80% in numerous plant species [1,7,10–12], however, the ability of plants to respond towards Cd stress depends on the tissue specificity of Cd toxicity; for example, leaf tissues accumulate more Cd than other root tissues and/or tuber vegetables [13]. Thus, there is a dire need to understand the tissue specificity of Cd toxicity and to remediate the soil and crops from Cd toxicity to reach a potentially win–win situation by deploying such amendments that not only increase the crop growth and its yield, but also detoxify the soils.

Many physical, chemical, and biological measures have been taken to minimize impacts of potentially toxic elements (PTEs) on the ecosystems [4,14]. Biochar (BC) is well known to be a highly recommended and effective material for ameliorating different environmental setbacks, including heavy metal pollution, owing to its environmental friendliness, widespread usage, and low cost [15,16]. BC has negative charge on its surface, along with high ion exchange ability, which means it can also effectively decrease translocation and phytoavailability of different PTEs, such as Ni, Cd, Cu, and Pb, in contaminated soils and in plants [17–19]. BC application improves heavy metal tolerance in plants by triggering numerous biochemical and physiological mechanisms, such as leaf gas exchange, accumulation of photosynthetic compounds, and oxidative damage [20]. However, recent studies showed that modification in BC with compost, synthetic fertilizers, and manures increases the potential of BC by many folds [21,22], for instance addition of sulfur modification in rice husk BC increased the BC mercury adsorptive capacity by ~73%, compared with no modification [23]. Likewise, modification of BC with mineral elements [24], phosphoric acid [25], or with biomaterials, such as chitosan [26], enhances soil properties and increases the oxygen-containing phenolic, carboxylic, and hydroxyl functional groups on soil surface, and thus converts more accessible forms of toxic ions into less accessible forms [25].

Iron is an important essential nutrient and its deficiency results in stunted growth and significant reduction in plant productivity [27]. Addition of iron (Fe) nanoparticles on BC surface can enhance the crop growth and its productivity [21]. Previous studies showed that Fe-BC reduced the bioavailability of heavy metal ions in soil and reduced the translocation of Cd, Cr, Pb, and Cu by 4.23–109.33% in heavy-metal-contaminated soil [25,28,29]. However, it has not been well examined yet how Fe-BC improves heavy metal tolerance in plants, thus the current study was carried out to reveal the possible role of Fe-BC in improving Cd tolerance in radish.

Heavy metal mobilization in soil is another concern while improving heavy metal tolerance in plants. BC application immobilizes PTEs via several reported mechanisms [30–33]. Modified BC increases the heavy metal immobilization [34]. For instance, compared to unmodified corncob BC, MgO-coated corncob BC reduced soil Pb leaching by 50.71%, as revealed by toxicity characteristic leaching procedure (TCLP) [33]. Likewise, rice husk BC modified with non-toxic elemental S reduced Hg concentrations in TCLP leachates by approximately 99% [35]. Thus, in this study, Fe-BC was applied to examine the Cd mobilization in soil and Cd translocation from root to shoot.

Heavy metal adsorption is an important mechanism and plays an important role in the immobilization of toxic ions in soil. In the current study, two models (Langmuir and Freundlich adsorption isotherm [36,37] were selected to observe the behavior of Cd adsorption on Fe-BC surface. The Langmuir model shows an ideal monolayer adsorption, which assumes that all adsorption sites have equal energies and absorbed molecules have no mutual interactions [38], while the Freundlich model is empirical in nature, and significant for only heterogeneous surface adsorption [39]. These models are well established and useful to examine the heavy metal adsorption capacity in soil with and without soil amendment. The interpretations of these models are based on their maximum adsorption capacity (q_{\max}), constant values (K_F/K_L), and its R^2 value, while here, q_{\max} shows the capacity of an adsorbent to capture the adsorbate on its surface to complete its mono-

layer [40]. For instance, the removal of Cu through *Rosa bourbonia* waste phytobiomass (RBWPB) biosorbent was estimated, and showed that the Langmuir isotherm model is best suited for Cu removal due to high maximum adsorption capacity of a material (q_{\max}) value (149.25 mg g^{-1}) [41]. Similarly, the adsorption capacity of Fe_2O_3 nanoparticles modified BC, and MgO-doped corn straw BC showed q_{\max} value of 94.34 mg g^{-1} and 160.03 mg g^{-1} for the removal of Cd and Cu (II), respectively [42,43]. Thus, current work was designed to study (i) the effect of Fe-BC on different physiological and biochemical parameters of radish under Cd stress; (ii) the role of Fe-BC in plant nutrition under Cd toxicity, and (iii) if there was Cd adsorption occur on Fe-BC soil, then isotherm models (Langmuir and Freundlich) were used to calculate the maximum Cd adsorption capacity on Fe-BC soil.

2. Materials and Methods

2.1. Iron Enriched Biochar

BC was prepared from wheat feedstock at a pyrolysis temperature of 500°C for 3 h in a furnace (TF-1200X). Later, this BC was ground, and passed through a 2 mm sieve. This BC was stored in a desiccator before use [44]. Iron doping was done by mixing the above-prepared BC in a mechanical vessel. The ratio between the BC and dry weight (DW) was 1:5 w/v . When the temperature reached 100°C , the iron chloride (FeCl_3) and iron sulphate (FeSO_4) were added (2:10 w/v) to the mixture. The homogenous mixture was attained after continuous mixing and heating. The BC was dried in the oven at 60°C to remove the excessive water from the BC mixture.

2.2. Pot Study

The study was conducted at a greenhouse (Government College University Botanical Garden, Lahore) located at $31^\circ33'20.54''$ N latitude and $74^\circ19'40.56''$ E longitude near Mall Road Lahore, Pakistan. Four treatments (control; Cd; Fe-BC; Cd+Fe-BC) along three replicates were chosen for this study. There were two level of Cd (0.75 mg kg^{-1}) and Fe-BC (0.0.5%), while the control treatment contained the pure clay loamy soil only. Pots were filled with 2 kg soil, and 10 seeds of *Raphanus sativus* L. (cultivar red radish) were sown per pot, with three replicates. After 8 days of germination, four plants per pot were maintained. Moisture concentration was maintained at 70% soil field capacity in all pots. Plants were harvested after 40 days, and various plant parts, such as root and shoot, were subjected to various physiological and biochemical analysis. After harvesting, fresh weights of root and shoot were calculated. After fresh weight calculation, these samples were placed into the oven at 70°C . After four days, the distilled water was calculated by subtracting the value of fresh weight from it.

2.3. Biochemical Analysis

Protein concentrations in root and shoot of radish plant were determined by following the method of [45]. Sample extract was prepared by taking 0.1 g of shoot/root samples, and ground by using 4 mL of 80% acetone. Then, 200 μL of sample extract was taken into a test tube and 1800 μL deionized water was added into it. Then, Bradford reagent (2 mL) was added, and the mixture was placed for incubation at room temperature for 10–20 min. After incubation, absorbance was measured at 595 nm wavelength by spectrophotometer (Shimadzu, UV-1201, Kyoto, Japan). Protein concentration (mg g^{-1} fresh weight) was measured by standard curve using different concentrations of bovine serum albumin (BSA).

Total phenolic in roots and shoots were colorimetrically measured by following Singleton et al. [46]. Reaction mixture (2 mL) was prepared by adding 20 μL of sample extract, 100 μL Folin–Coicâlteu's reagent (0.25 N), deionized water (1580 μL), and 300 μL Na_2CO_3 (1 N). The mixture was placed in the dark at room temperature for 2 h. Absorbance of sample mixture and gallic acid standards were measured at 760 nm on spectrophotometer (Shimadzu, UV-1201, Kyoto, Japan). The concentration of total phenolic was presented in $\mu\text{g g}^{-1}$.

Chlorophyll concentration was measured by using fresh, fully expanded leaf material; 1 g leaf sample was ground with the help of pestle and mortar in 90% acetone. Absorbance was measured on UV-Vis spectrophotometer (Shimadzu, UV-1201, Kyoto, Japan) by using the following equations:

$$\text{Chl. a (mg mL}^{-1}\text{)} = 11.64 \times (\text{A663}) - 2.16 \times (\text{A645}) \quad (1)$$

$$\text{Chl. b (mg mL}^{-1}\text{)} = 20.97 \times (\text{A645}) - 3.94 \times (\text{A663}) \quad (2)$$

(A663) and (A645) represent absorbance values read at 645 and 663 nm wavelength, respectively [47].

Malondialdehyde (MDA) concentration was measured by adding 5 mL of 20% trichloroacetic acid solution into the paste of fresh leaf (0.1 g). The mixture was centrifuged at 10,000 rpm for 15 min. The collected supernatant (2.5 mL) was taken, and 1 mL of both solutions trichloroacetic acid (20% *v/w*) and thiobarbituric acid (0.5% *v/w*) added in it. The solution was placed in an oven at 95 °C for 30 min and then cooled in a water bath. Absorbance for MDA was measured at 532 and 600 nm wavelengths by using the Beer-Lambert equation [48].

Cell membrane permeability (CMP) was measured by adding fresh leaf (0.1 g) into the test tubes containing 5 mL of distilled water. Test tubes were placed on a shaker for 4 hrs. Electrical conductivity (EC) of the solution was measured with an EC meter. Then, samples were autoclaved at 121 °C for 20 min. The solution was cooled down to room temperature and a second reading of EC was taken. The first reading was divided by the second reading and multiplied by 100 to measure CMP [48].

2.4. Crude Leaf Extract for Antioxidant Enzyme Assays

Fresh leaf tissues (0.2 g) were taken and ground to a fine powder using pestle and mortar. The exact weight of each powdered sample was measured before it was thoroughly homogenized in 1.2 mL of 0.2 M potassium phosphate buffer (pH 7.8; 0.1 mM ethylene di-amine tetra acetic acid). The sample was centrifuged at $15,000 \times g$ for 20 min at 4 °C. The supernatant was removed from the sample, and pellet resuspended in 0.8 mL of the same buffer. This suspension was centrifuged for another 15 min at $15,000 \times g$. The combined supernatant was stored in the freezer and used to measure different antioxidant enzyme activities.

Reaction mixture (3 mL) containing 2 mL enzyme extract (diluted 200 times with 50 mM, 7.0 pH potassium phosphate buffer) and 1 mL H_2O_2 (10 mM) was measured on a spectrophotometer (Shimadzu, UV-1201, Kyoto, Japan). Catalase (CAT) activity was measured at 240 nm in mol unit activity $\text{min}^{-1} \text{mg}^{-1}$ protein at 25 ± 2 °C [49].

Ascorbate peroxidase (APX) activity was measured by modified method of Nakano and Asada [50]. It was measured from the decrease in absorbance at 290 nm due to oxidation of ascorbate in reaction. Assay mixture (1 mL) was prepared by following protocol: 50 mM potassium phosphate buffer (pH 7), 0.5 mM H_2O_2 , 0.5 mM ascorbate, and 10 μL of crude leaf extract. H_2O_2 was added to initiate the reaction mixture and decrease in absorbance was measured for 3 min on a spectrophotometer (Shimadzu, UV-1201, Kyoto, Japan). The extinction coefficient of $2.8 \text{ mM}^{-1} \text{ cm}^{-1}$ for the reduced ascorbate was used in measuring enzyme activity that was expressed in terms of mol unit activity $\text{min}^{-1} \text{mg}^{-1}$ protein.

2.5. Nutrients and Heavy Metal Analysis

The roots and shoots of radish plant were air dried and then placed in the oven at 70 °C for two days. Dried plant samples were digested with $\text{HNO}_3 + \text{HClO}_4$ (2:1) for analysis of Fe, Na, K, Ca, Mg, and Cd on multi-sequential atomic absorption spectrophotometer (ISE-3000 series) by using Jones et al. [51].

To determine soil Cd concentration, calcium chloride (CaCl_2) (1.1 g) and diethylene-triamine pentaacetic acid (DTPA) (1.97 g) were taken into a beaker. Deionized water was

used to dissolve these salts. Triethanolamine (TEA) was added into another beaker. The pH was adjusted to 7.3 with 6 N HCl and brought to 1 L. This solution had CaCl_2 , 0.005 M DTPA, and 0.1 M TEA. Standards for Cd determination in soil were prepared and analyzed on a multi-sequential atomic absorption spectrophotometer [51].

2.6. Biosorption Analysis

The total amount of metal absorbed onto absorbent was calculated by the method of simple difference in concentration. The biosorption capacity of Fe-BC for Cd was estimated using the concentration of ions retained on a unit mass of absorbent by using Equation (3) [52].

$$q = (C_e - C_i) \times (V/1000)/m \quad (3)$$

where C_i is the initial concentration of cadmium (mg kg^{-1}), C_e is the final concentration (mg kg^{-1}), V is the volume of solution (mL), and m is the biosorbent mass (g).

The percentage removal efficiency was determined according to Equation (4)

$$\% \text{ removal} = C_e - C_i / C_e \times 100 (\%) \quad (4)$$

Definite parameters (isotherm models) are used to determine the biosorption isotherms, whose values show the affinity of biosorbent for various heavy metal ions, along with the surface properties [52]. In our study, Langmuir and Freundlich isotherms were used to fit the experimental data. The mathematical expressions of log form of Freundlich isotherm and linearized form of Langmuir equation are represented in Equations (5) and (6), respectively.

$$C_e/q_e = 1/q_{\max}K_L + C_e/q_{\max} \quad (5)$$

$$\text{Log } q_e = 1/n (\text{Log } C_e) + \text{Log } K_F \quad (6)$$

Here, q_e shows metal ion (Cd) sorbed (mg kg^{-1}), K_L is Langmuir equation constant, and K_F and $1/n$ are the Freundlich equation constants, respectively.

2.7. Statistical Analysis

Statistical analysis of data was performed by using Microsoft Excel 2010® (Microsoft Cooperation, Redmond, WA, USA) and *Statistix 8.1*® software package (Copyright 2005, Analytical Software, USA) [53]. Least significant difference (LSD) at $p < 0.05$ was determined by taking the difference between any two treatment means [54].

3. Results

3.1. Fe-Rich Biochar Improves Radish Growth and Nutrient Uptake under Cd Stress

Cadmium (Cd) stress significantly ($p < 0.01$) reduced root biomass accumulation (Table 1). The Cd stress decreased root dry weight (RDW) by 85% and shoot dry weight (SDW) by 30%, relative to control. Fe-BC minimized the toxic effect of Cd on biomass accumulation by improving RDW and SDW up to 21-fold and three-fold, respectively, compared with no Fe-BC application under Cd stress (Table 1).

Cd significantly reduced the uptake of Ca in both root and shoot, compared with control, while no significant effects of Cd toxicity were observed in the uptake of K, Na, Mg, and Fe in root and shoot, except Na in shoot, which reduced by 86% in shoot under Cd toxicity (Table 1), compared to Cd+Fe-BC. However, the treatment of Fe-BC treatment, along with Cd stress, significantly diminished the effects of Cd stress on plant nutrition by improving the uptake of Ca, Mg, K, Na, and Fe in root and shoot (Table 1). The maximum increase (twofold) in shoot Ca concentration was found in combined treatment of Cd+Fe-BC, compared to Cd stress. Fe-BC application, along with Cd stress, improved Mg (twofold and twofold) and K (13-fold and twofold) uptake in root and shoot, respectively, compared with Cd stress only (Table 1). Fe-BC treatment, along with Cd, increased Fe uptake by twofold in root only, compared with Cd stress only (Table 1).

Table 1. Status of macro- and micronutrients in root/shoot of radish cultivar under different treatments (control; Cd; Fe-biochar (BC); Cd+ Fe-BC). Concentrations of sodium (Na), calcium (Ca), potassium (K), and iron (Fe) were determined from both root and shoot of radish cultivar after harvesting.

Treatment	Root						Shoot					
	DW	Ca	Mg	K	Na	Fe	DW	Ca	Mg	K	Na	Fe
	g		mg g ⁻¹			mg kg ⁻¹	g		mg g ⁻¹			mg kg ⁻¹
Control	0.07 ± 0.01b	0.59 ± 0.11c	0.22 ± 0.03c	0.03 ± 0.01b	0.48 ± 0.01b	37.9 ± 11.1b	0.1 ± 0.02ab	1.94 ± 0.06a	0.5 ± 0.03a	0.18 ± 0.07a	1.28 ± 0.07b	37.9 ± 11.1a
Cd	0.01 ± 0.03c	0.42 ± 0.13d	0.19 ± 0.06c	0.01 ± 0.03b	0.49 ± 0.11b	71.4 ± 22.3b	0.07 ± 0.01ab	0.99 ± 0.001c	0.2 ± 0.04b	0.14 ± 0.07b	0.92 ± 0.09c	49.1 ± 22.3a
Fe-BC	0.2 ± 0.01a	2.39 ± 0.09a	0.47 ± 0.03a	0.08 ± 0.07b	0.60 ± 0.02b	82.5 ± 11.1b	0.27 ± 0.01a	1.40 ± 0.13b	0.3 ± 0.03b	0.49 ± 0.03c	1.72 ± 0.02a	60.2 ± 11.1a
Cd+Fe-BC	0.22 ± 0.07a	2.17 ± 0.57b	0.49 ± 0.15b	0.14 ± 0.05a	0.93 ± 0.09a	171.8 ± 11.1a	0.20 ± 0.04a	2.10 ± 0.08a	0.6 ± 0.08a	0.35 ± 0.02d	0.72 ± 0.09d	71.4 ± 22.3a
LSD _{0.05}	0.03	0.15	0.06	0.09	0.16	46.48	0.17	0.2	0.06	0.04	0.17	26.83

Mean values showing different letters are significantly different ($\leq p \leq 0.05$) from each other.

3.2. Fe-Rich Biochar Reduces Membrane Permeability by Improving Antioxidant Defence System

CMP and MDA were significantly ($p < 0.01$) enhanced upon Cd stress (Figure 1A,B). A twofold increase in CMP production was observed with Cd stress, compared to control. However, Cd+Fe-BC application decreased (55%) CMP relative to Cd stress (Figure 1A). A similar pattern was observed in MDA, where Cd stress increased (36%) MDA relative to control. However, Fe-BC showed maximum decrease (48%) in MDA when added in a combined form of Cd+Fe-BC treatment, compared to Cd stress (Figure 1B). Cd-stress-induced oxidative damage was significantly reduced by the activation of antioxidants in response to Fe-BC application (Figure 2A,B). APX and CAT activities were increased by 32% and five-fold under Cd stress, compared with control. However, Cd+Fe-BC treatment increased APX activity by 92%, compared with Cd stress only, but did not show any significant difference on CAT activity, suggesting the specificity of the regulation of antioxidant in response to Fe-BC under Cd stress (Figure 2A,B).

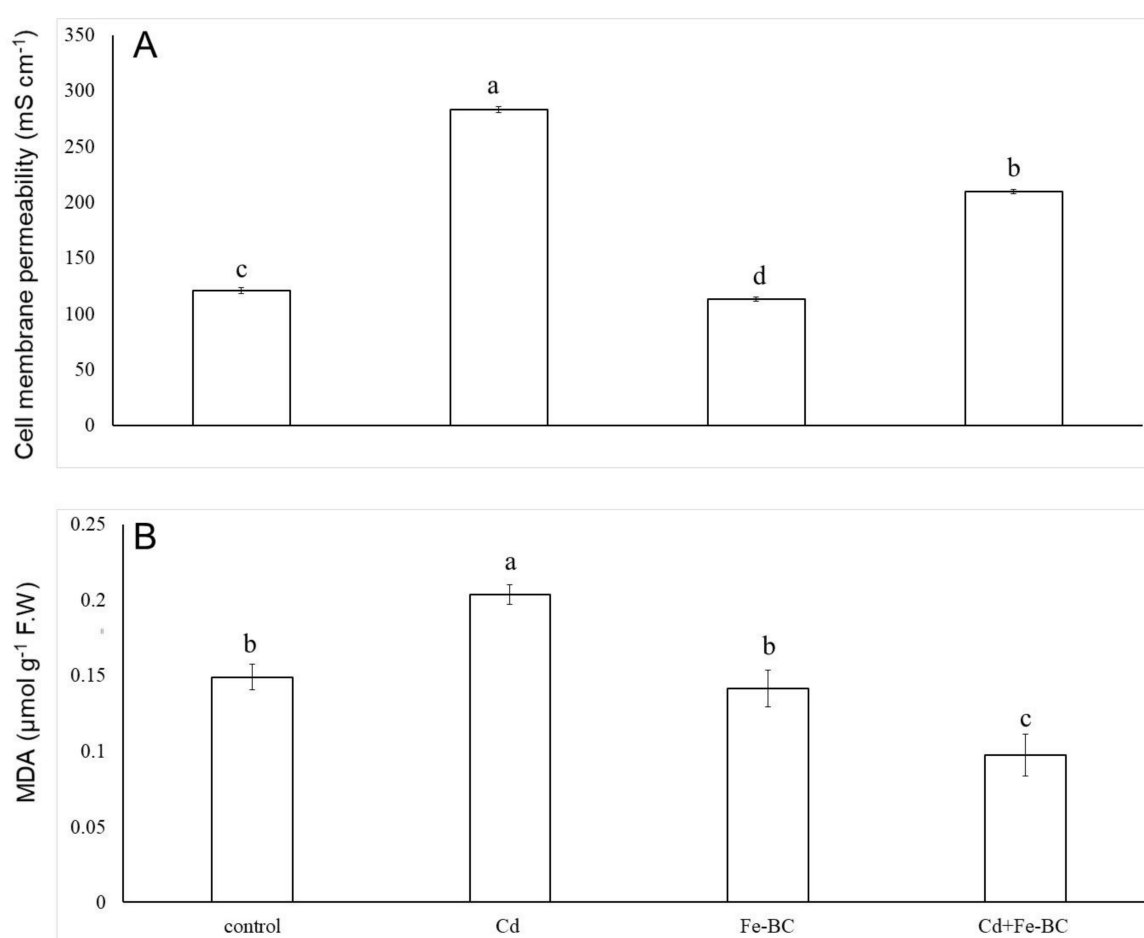


Figure 1. Cell membrane permeability (A) (mS cm⁻¹) and malondialdehyde (MDA) (B) (μmol g⁻¹ F.W.) concentration of radish cultivar grown under various treatments (control, Cd, Fe-BC, Cd+Fe-BC). There were three repeats/treatment. Values are the average of three replicates ± standard error of mean (SEM).

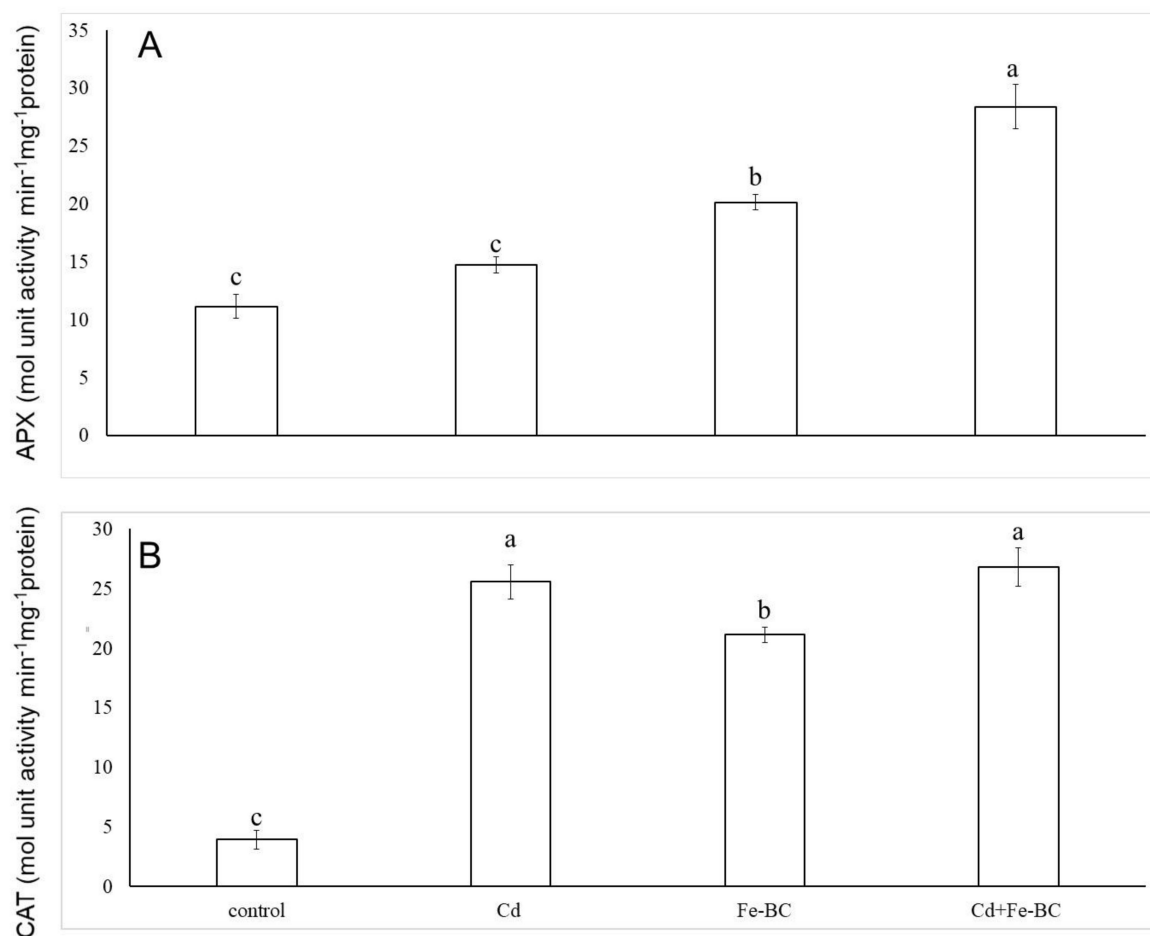


Figure 2. Ascorbate peroxidase (APX) (A) and catalase (CAT) (B) activities (mol unit activity min⁻¹ mg⁻¹ protein) of radish leaves grown under various treatments (control, Cd, Fe-BC, Cd+Fe-BC). There were three repeats/treatment. Values are the average of three replicates \pm SEM.

3.3. Fe-Rich Biochar Improves Osmolytes Accumulation and Photosynthetic Pigments under Cd Stress

Total root phenolic was highly significant ($p < 0.01$) by interactive effects of treatments. There was a significant ($p < 0.01$) decrease in total root phenolic observed with Cd stress, compared to Fe-BC treatment (Figure 3A). However, combined treatment of Cd+Fe-BC increased the total root phenolic contents up to 7%, compared to Cd stress only. Similarly, radish cultivar showed reduction (13%) in total shoot phenolic observed under Cd stress relative to Cd+Fe-BC treatment (Figure 3B).

Cd stress significantly influenced ($p < 0.01$) total root/shoot protein concentration by all the treatments and decreased total root protein concentration, compared to control (Figure 3C), while it was observed that total root protein increased significantly by the combined application of Cd+Fe-BC relative to Cd stress. However, total shoot protein showed the same behavior; when Cd stress applied it decreased (11%), compared to control (Figure 3D).

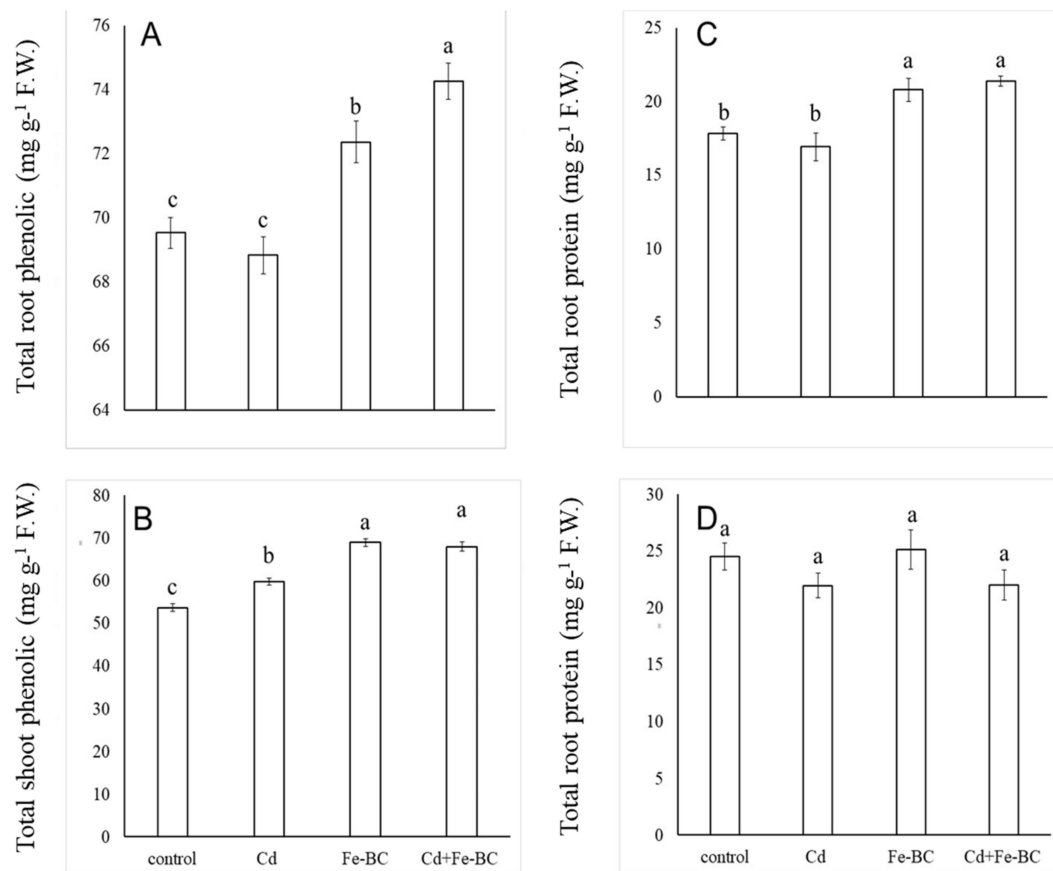


Figure 3. Total root phenolic (A) and total shoot phenolic (B) (mg g^{-1} F.W.) of radish cultivar grown under various treatments (control, Cd, Fe-BC, Cd+Fe-BC). There were three repeats/treatment. Values are the average of three replicates \pm SEM. Total root protein (C) and total shoot protein (D) (mg g^{-1} F.W.) of radish cultivar grown under various treatments (control, Cd, Fe-BC, Cd+Fe-BC). There were three repeats/treatment. Values are the average of three replicates \pm SEM.

Cd stress reduces the biosynthesis of chlorophyll concentrations in leaves. Chlorophyll a and b were decreased by 24% and 30%, respectively, in response to Cd stress, compared with control (Figure 4). However, Cd-induced decline in chlorophyll concentrations were ameliorated by the application of Fe-BC, suggesting a protective role of Fe-BC in radish under Cd toxicity. Fe-BC increased chlorophyll a and b significantly by 30% and 52% under Cd stress, compared with Cd stress only (Figure 4).

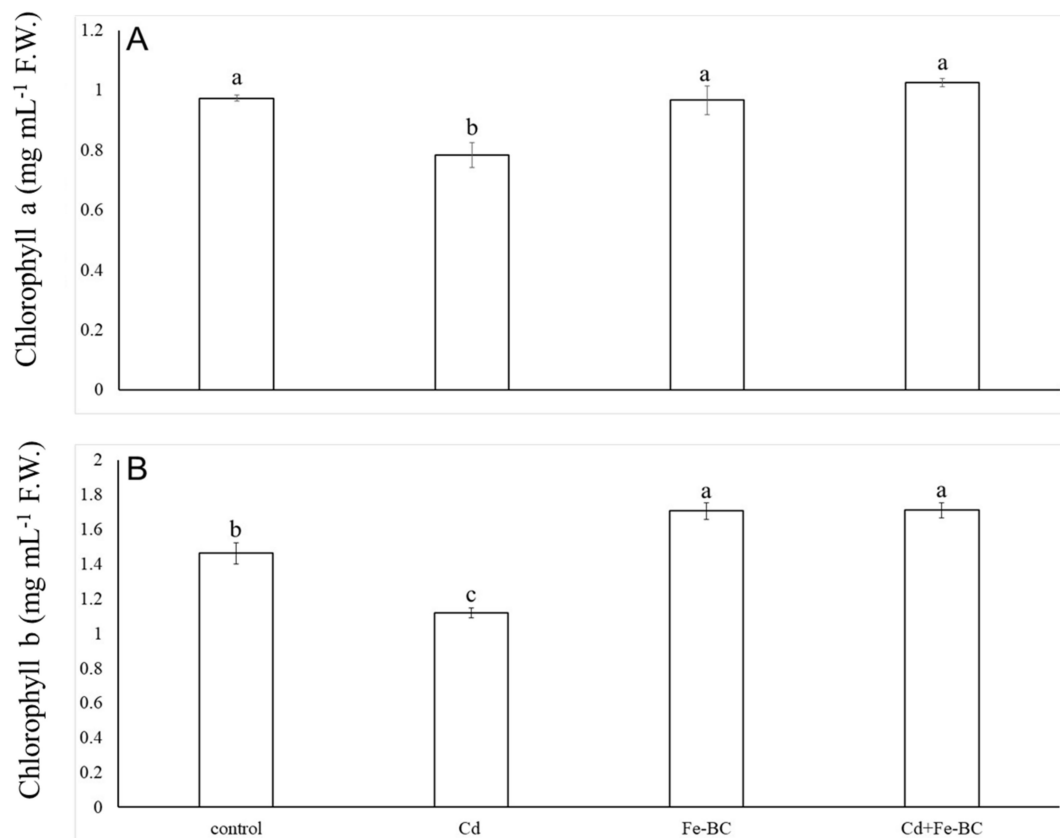


Figure 4. Chlorophyll a (A) and b (B) concentrations (mg mL⁻¹ F.W.) of radish cultivar grown under various treatments (control, Cd, Fe-BC, Cd+Fe-BC). There were three repeats/treatment. Values are the average of three replicates \pm SEM.

3.4. Soil Cd, Langmuir and Freundlich Models

Fe-BC application in the presence of Cd stress reduced root Cd concentration about 12-fold, compared to Cd stress only. This result clearly showed that application of Fe-BC helped in diminishing the negative impact of Cd stress on radish cultivar and reduced its translocation from root to shoot (Table 2).

Table 2. Cd concentration in root and shoot, along with diethylenetriamine pentaacetic acid (DTPA)-extractable Cd in soil under different treatments (control, Cd, Fe-BC, Cd+ Fe-BC) were measured after harvesting of radish cultivar.

Parameters	Root Cd mg g ⁻¹	Shoot Cd mg g ⁻¹	DTPA-Extractable Cd in Soil mg kg ⁻¹
Control	n.d. *	n.d. *	1.21 \pm 0.30
Cd	0.0257 \pm 0	0.005 \pm 0.04	1.86 \pm 0.06
Fe-BC	n.d. *	n.d. *	0.78 \pm 0.30
Cd+Fe-BC	0.002 \pm 0.02	n.d. *	1.21 \pm 0.30

* n.d. = not detected.

While it was noticed that the extractable DTPA-Cd was more reduced (34%) in combined treatment of Cd+Fe-BC than Cd stress only, addition of Fe-BC restricted the transfer of Cd in root and shoot to a not-detectable level (Table 2). However, interpretation of Langmuir and Freundlich models suggested that R² and q_{max} value supports the Langmuir isotherm model for the adsorption of Cd concentration (Table 3).

Table 3. Comparison between Langmuir and Freundlich isotherm for Cd ions biosorption onto Fe-BC under various treatments (control, Cd, Fe-BC, Cd+Fe-BC). The best model was selected based on Cd adsorption on soil–Fe-BC interface, represented as R^2 and q_{\max} values. See text for further interpretation.

Biosorbent	Freundlich			Langmuir			
	K_F mg kg^{-1}	$1/n$	R^2	q_e mg kg^{-1}	$X_m q_{\max}$ mg kg^{-1}	K_L mg kg^{-1}	R^2
Control	0.1194	0.437	0.9951	2.6422	0.6608	3.6616	0.9993
Cd	0.788	0.0276	0.9983	0.3358	2.1786	8.470	0.9982
Fe-BC	0.1254	0.3962	0.9989	2.6621	4.9904	1.00001	0.9998
Cd+Fe-BC	0.9059	0.2879	0.9517	1.4707	9.9786	9.7276	0.9991

4. Discussion

4.1. Iron-Rich Biochar Maintained Cell Membrane Stability by Triggering Antioxidant Defence System and Osmolyte under Cd Stress

Plants usually maintain balance between reactive oxygen species (ROS) generation and its removal under normal growth conditions; however, this stability is disturbed under stress conditions [6,54]. Under stress condition, a burst of ROS is responsible for lipid peroxidation, which ultimately leads to CMP on the cell membrane [55,56]. Membrane damage was measured indirectly through electrical conductivity of solute leakage from the plant cell; as shown in the present study, where CMP was increased under Cd stress (Figure 1A). Plasma membrane could be damaged due to various mechanisms, such as the oxidation reaction from ROS, resulting in an increase in CMP, which further enhances the non-selective ion conductance across the cell membrane [57]. It minimizes the activity of H^+ -ATPase of plasma membrane, probably due to change in fluidity and composition of membrane lipids. Mishra et al. [58] reported that Cd, similar to the other classes of metals, has a strong attraction towards sulfur (S)- and nitrogen (N)-containing proteins and ligands. Thus, it binds within proteins leading to disturbed membrane ion channels and ion leakage. However, such negative impacts of Cd stress on CMP and lipid peroxidation was ameliorated by the Fe-BC application (Figure 1A). Fe-BC application reduced CMP and MDA concentrations by 25% and 52%, respectively, under Cd stress, compared with Cd stress only (Figure 1A,B), suggesting that Fe-BC could improve Cd tolerance in radish by maintaining CMP. BC can diminish the oxidative stress by lowering the production of reactive oxygen species and enhancing the antioxidant activities in plant leaves [54]. When antioxidant increases in response to application of BC, it helps in preventing the initiation or proliferation of oxidizing chain responses, which results in delay or inhabitation of oxidation in plant cells, protein, lipids, and other essential molecules [59].

As an adaptive response, the excessive ROS production is tightly controlled by the activation of antioxidants; though it is not necessary that high antioxidant activity leads to higher ROS detoxification [60]. In the current study, CAT and APX activities were regulated in response to Fe-BC application under Cd stress. Fe-BC application did not affect the CAT activity, but it enhanced APX activity (Figure 2B), which was negatively correlated with MDA concentrations and positively correlated with higher root and shoot biomass accumulation under Cd stress (Table 4). Our results suggest that Fe-BC was able to activate or trigger only heme-based APX enzyme, due to its Fe-richness and higher Fe uptake under Cd stress. Our results are, in contrast with Mohamed and Aly [61], that Fe deficiency reduced the CAT and APX activity by 49% and 53%, respectively. However, it has been shown that Fe regulates the expression of cytosolic APX enzyme activity by the activation of the *APX1* gene [62,63]. Thus, it can be suggested that Fe-BC maintains redox homeostasis by regulating peroxidase enzyme activity.

Table 4. Pearson coefficient correlation drawn between the radish dry weight and its physiological and biochemical parameters.

	CMP	MDA	APX	CAT	Total Root Phenolic	TRP	TSP	Chl a	Chl b	Total Shoot Phenolic	RDW
MDA	0.2773										
APX	0.0811	−0.7376 **									
CAT	−0.5720 *	−0.1369	0.6464 *								
Total root phenolic	−0.2106	−0.7745 **	0.8945 **	0.3861							
TRP	−0.3777	−0.7020 **	0.6899 **	0.2769	0.7753 **						
TSP	−0.5423	0.1428	−0.4083	−0.4057	−0.2044	0.2045					
Chl a	−0.4664	−0.9051 **	0.5930 *	−0.0510	0.6835 **	0.5642 *	0.0128				
Chl b	−0.6177 *	−0.7853 **	0.6744 **	0.0926	0.7725 **	0.8740 **	0.1791	0.7359 **			
Total shoot phenolic	−0.2479	−0.5678 *	0.7377 **	0.6069*	0.6948 **	0.7633 **	0.0428	0.5120	0.7325 **		
RDW	−0.5150	−0.8375 **	0.7602 **	0.2434	0.8772 **	0.8833 **	0.1127	0.7857 **	0.9459 **	0.8256 **	
SDW	−0.7988 **	−0.3926	0.2593	−0.0329	0.4545	0.5952 *	0.3900	0.4585	0.7324 **	0.6767 **	0.7501 **

CMP—Cell membrane permeability; MDA—Malondialdehyde; APX—Ascorbate Peroxidase; CAT—Catalase; TRP—Total root protein; TSP—Total shoot protein; Chl a—Chlorophyll a; Chl b—Chlorophyll b; RDW—Root dry weight; SDW—Shoot dry weight, * Significant at $p \leq 0.05$, ** highly significant at $p \leq 0.01$.

4.2. Iron-Rich Biochar-Induced Radish Growth Improvement was Due to Higher Chlorophyll Concentrations under Cd Stress

Cd-induced oxidative stress not only affects the defense systems of plants, but also reduces photosynthetic capability of plants [10]. Cd stress reduces chlorophyll concentrations by altering chloroplast structures, disrupted biosynthesis of chlorophyll, and oxidative damage to the growth of photosynthetically active cell in leaves [64]. In the current study, chlorophyll a and b concentrations were significantly reduced by Cd stress (Figure 4), which can be a direct result of Cd toxicity on chlorophyll biosynthesis [65] and minimized carotenoids concentration. The carotenoids are known to protect the chlorophyll and other vital macromolecules by reducing excited triplet state of chlorophyll to avoid the formation of free radicals. However, in the current study, Fe-BC-induced radish growth improvement was due to higher accumulation of chlorophyll concentrations under Cd stress (Figure 4). Similar results are reported by Liu et al. [66] that moderate Fe supplementation increases the photosynthesis capacity by increasing leaf gas exchange and the activation of photosystems I and II. Fe-BC-induced increase in chlorophyll concentrations in radish was positively correlated with Fe-BC-induced activation of APX activity and reduced ROS production (Table 4). As stated above, APX belongs to the heme-containing peroxidase enzyme family, and underlying mechanisms behind Fe-BC-induced higher APX activity could be associated with higher Fe uptake. A strong and positive correlation was also found between chlorophyll concentrations and RDW and SDW in response to Fe-BC treatment under Cd toxicity (Table 4), suggesting the ameliorative role of Fe-BC in inducing Cd tolerance in radish by protecting/stimulating chlorophyll concentrations. Previously, BC application increased the chlorophyll concentrations in numerous plant species under metal stresses [67,68]. BC-amended soil has the ability to enhance N mineralization of soil and absorb NH_4^+ more than NO_3^- on its surface, ensuring more N availability for uptake and growth of the plant. In *Silybum marianum*, potassium-doped BC improves the photosynthesis process by enhancing the synthesis of chlorophyll pigments in plants, and water-holding capacity of soil under drought stress [69].

The reduction in chlorophyll concentration is a result of the replacement of Mg with Cd ions in chlorophyll molecules, as the conversion of chlorophyll to pheophytin percentage enhances with an increase in Cd stress [70]. In the current study, Fe-BC treatment increased Mg concentrations in root and shoot under Cd stress, further explaining the underlying mechanism of higher chlorophyll concentrations in radish under Cd toxicity in response to Fe-BC treatment. Iron is also essential for chlorophyll biosynthesis, and the synthesis of heme and its deficiency significantly impairs plant growth and development [71]; this further explains the increase in chlorophyll concentrations in response to Fe-BC under Cd toxicity.

4.3. Biochar Improves Biomass Accumulation and Plant Nutrition under Cd Stress

Cd toxicity reduces plant growth and development by reducing the morphological and physiological growth of plants, as observed in numerous plant species [72,73]. In the present study, root and shoot dry biomass of radish was decreased by Cd toxicity up to 85% and 30%, respectively, compared with control. Reduction in radish root and shoot biomass production was associated with elevated Cd-induced oxidative damage, altered nutrient uptake, and production of photosynthetic pigments (Table 1). Similar results have been reported in multiple studies, indicating Cd reduces plant growth by altering these physiological mechanisms [66,68,74]. However, Fe-BC application improved RDW and SDW under Cd toxicity, which was positive and strongly correlated with higher nutrient uptake, chlorophyll concentrations, and higher ROS detoxification [75].

Cd interferes with the uptake of numerous essential elements, and thus disrupts ionic homeostasis in plants [76]. In the current study, Cd toxicity reduced the uptake of K, Ca, Mg, and Na, however, Fe-BC treatment improved the uptake of these elements under Cd stress (Tables 1 and 2). Possible explanations can be suggested here that (i) Fe-BC increased root penetration (as observed in terms of higher RDW) and concomitantly increased the

uptake of nutrients from soil solution [77], (ii) the presence of different groups (carboxylic and phenolics) on the Fe-BC surface can significantly improve the water-holding capacity, cation exchange capacity, and nutrient uptake and retention [78,79], and (iii) such modified BC can slow down the cation loss by inducing a shift in transport of soil water nutrient from bypass to matrix flow [80]. The current study also showed that radish roots have higher concentrations of Cd than in shoots of radish plant (Table 2), suggesting the translocation of Cd in radish was tightly regulated, and retained excess Cd in radish root system without causing damage [81]. Cd transport in plants is mediated by several ion transporters, such as low-affinity cation transporter [82], members of the natural resistance-associated macrophage protein (NRAMP) family [83], zinc/iron-regulated transporter-like proteins (ZIPs) [84], and IRT1 (Fe-regulated transporter) [85]. The activities of these transporters are tightly regulated and are greatly influenced in the presence of iron [71,86–88]. For instance, in rice, Cd accumulation in root is primarily due to higher expression of *OsHMA3* [83] and thus poses more Cd transportation to the vacuoles [89]. In *Arabidopsis*, NRAMP genes encode metal transporters, and AtNRAMPs transport both the metal nutrient Fe and the toxic metal Cd [90]. Likewise, in rice, the expression of NRAMP tightly controlled the iron and Cd acquisition in root and shoot, and the suppression of *OsNRAMP5* promoted Cd translocation to shoots, thus indicating an important role of NRAMP in regulating Fe and Cd transportation. Though the expression analysis of these ion transporters were not conducted in this study, it can be suggested, from these findings, that Fe-BC improves Cd tolerance in plants by regulating the expression of these transporters in roots.

Cd presence in plant root can significantly alter the plant metabolism; hence disturbance occurs in uptake and transportation of nutrients (Ca^{2+} , K^+ , Mg^{2+} , and Fe^{2+}) from root to shoot [91] (Tables 1 and 2). There might be some possible fate of Cd while interacting with Fe-BC and plant roots: (i) interaction initiated either by competition with other cations for the binding sites on soil/Fe-BC particles; (ii) sometimes, Cd has the same routes of transportation or transporter families, such as NRAMP and ZIP/IRT, which play an important role in transport of mineral nutrients [92,93], (iii) similarly; a possible mechanism of Cd-induced disturbance in ion balance is initiated that is the competition of Cd for Ca^{2+} transporters. It causes an inducible deficiency (the deficiency of essential metals in plants) [94]. The struggle between Cd and other nutrients for the same transporters, minimizing the availability of Cd by enhancing its precipitation and adsorption on soil/Fe-BC surface, along with the sequestration of Cd in cell compartments inside the plant, shows the direct impact of nutrients on Cd bioavailability [95].

4.4. Soil Cd and Langmuir and Freundlich Models

The extractable DTPA-Cd was reduced (53%) in combined treatment of Cd+Fe-BC (Table 2), which was confirmed by previous research [96,97]. The above pot study suggested that the decrease in Cd was due to the addition of sulfur-iron-modified BC, which helped in preventing the mobilization of Cd in soil [98], as Fe-BC shows more thermal stability, functional groups, and larger surface area than pristine BC [99]. Moreover, sulfur Fe-BC has a synergetic impact on soil Cd; it possibly causes hydrolysis of Fe and produces Fe $(\text{OH})_2$ and other ageing products, such as goethite, which restricts Cd transportation in soil. It also produces positive charged hydroxyl Fe complexes, such as $\text{Fe}(\text{OH})_3$, $\text{Fe}(\text{OH})^{2+}$, $\text{Fe}_2(\text{OH})_2^{4+}$, $\text{Fe}_3(\text{OH})_4^{5+}$, $\text{Fe}(\text{OH})^{4+}$, and $\text{Fe}_2(\text{OH})_2$ [96], and, moreover, precipitation and coagulation of soil mineral colloids, e.g., negatively charged mineral colloids, such as kaolinite, quartz, montmorillonite, and glimmerton. These substances increase adsorption capacity of PTEs, such as Cd, by isomorphous replacement or attachment with modified BC [97].

Adsorption pattern of Cd was analyzed with two adsorption isotherm models, in which the Langmuir isotherm model displayed a better trend than the Freundlich isotherm model, as it showed higher R^2 and q_{max} values [100] (Table 3). The Langmuir isotherm model showed that the adsorption sites are homogenous, with monolayer coverage of Cd ions on the outer surface of biosorbents (Table 3). There was maximum Cd sorption

capacity (q_{\max}) increased from 2.178 to 9.976 with Cd+Fe-BC application relative to Cd only (Table 3). The electrostatic interaction or complexation of Fe-BC with Cd highlighted the metal immobilization, as discussed in our study (Table 3) [101]. With Fe coating on BC, the maximum As (III) sorption capacity increased from 19 to 31 mg g⁻¹, while As (V) sorption increased from 5.5–7.1 to 15–16 mg g⁻¹. He et al. [102] showed that Fe-BC removed As (V) by 6.8 mg g⁻¹, compared to unmodified BC, which shows adsorption capacity of 0.017 mg g⁻¹. The possible sorption mechanism was through As complexation with Fe³⁺ on the BC surface [103]. Moreover, the adsorption mechanism by Fe-BC is affected by the change of oxidation state of any metal in organic matter, such as ferrous to ferric (as revealed by π - π interaction in this study), ion exchange, surface adsorption, electrostatic interactions, surface complexation, and metal precipitation [104–107].

5. Conclusions

The current study revealed the positive role of Fe-BC in improving Cd tolerance in plants (Figure 5). BC made from wheat straw and doped with Fe decreases CMP by increasing osmolyte accumulation and by the activation of antioxidant activity. Moreover, Fe-BC improves plant mineral nutrition and photosynthetic pigment accumulation by reducing the translocation of Cd from root to shoot. Fe-BC treatment showed higher q_{\max} value than all other treatments, which intimated that Fe-BC was an excellent biosorbent for Cd. The current results are very useful in designing or understanding the underlying mechanism of BC-induced heavy metal tolerance in plants.

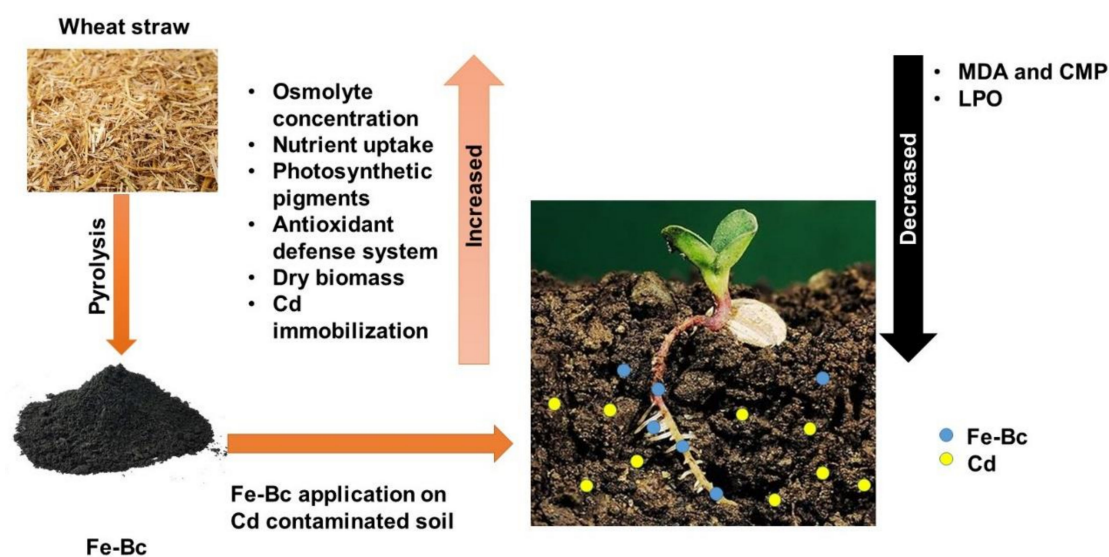


Figure 5. A graphical summary of the current study; biochar was made from wheat straw and doped with iron to improve BC productivity. Fe-BC improves Cd tolerance in radish by reducing the Cd translocation from root to shoot, by improving photosynthetic pigment accumulation and plant mineral nutrient and biomass accumulation. Fe-BC also improved Cd tolerance by regulating redox regulation.

Author Contributions: W.-u.-D.K. conceived the idea and designed the research. F.P.D. and P.M.A.R. conducted the experiment and analyzed the data. F.P.D., W.-u.-D.K., M.T., R.S., and A.M. developed the full draft and analyzed the data. W.-u.-D.K. and M.T. revised and critically reviewed the manuscript. All authors contributed to the subsequent development and approved the final manuscript. At the end, all authors again reviewed the manuscript carefully. All authors have read and agreed to the published version of the manuscript.

Funding: The authors are grateful to Punjab Agriculture Research Board for the financial support by research funds (grant number 894).

Conflicts of Interest: The authors declare no conflict of interest.

References

1. Anjum, S.A.; Ashraf, U.; Tanveer, M.; Khan, I.; Hussain, S.; Shahzad, B.; Wang, L.C. Drought induced changes in growth, osmolyte accumulation and antioxidant metabolism of three maize hybrids. *Front. Plant Sci.* **2017**, *8*, 69. [\[CrossRef\]](#) [\[PubMed\]](#)
2. Jiang, L.; Tanveer, M.; Han, W.; Tian, C.; Wang, L. High and differential strontium tolerance in germinating dimorphic seeds of *Salicornia europaea*. *Seed Sci. Technol.* **2020**, *48*, 231–239. [\[CrossRef\]](#)
3. Shah, A.N.; Tanveer, M.; Hussain, S.; Yang, G. Beryllium in the environment: Whether fatal for plant growth? *Rev. Environ. Sci. Biotechnol.* **2016**, *15*, 549–561. [\[CrossRef\]](#)
4. Shahzad, B.; Tanveer, M.; Che, Z.; Rehman, A.; Cheema, S.A.; Sharma, A.; Zhaorong, D. Role of 24-epibrassinolide (EBL) in mediating heavy metal and pesticide induced oxidative stress in plants: A review. *Ecotoxicol. Environ. Saf.* **2018**, *147*, 935–944. [\[CrossRef\]](#)
5. Tanveer, M.; Yousaf, U. Plant single-cell biology and abiotic stress tolerance. In *Plant Life under Changing Environment*; Academic Press: Cambridge, MA, USA, 2020; pp. 611–626.
6. Tanveer, M.; Hasanuzzaman, M.; Wang, L. Lithium in Environment and Potential Targets to Reduce Lithium Toxicity in Plants. *J. Plant Growth Regul.* **2019**, *38*, 1574–1586. [\[CrossRef\]](#)
7. Anjum, S.A.; Tanveer, M.; Hussain, S.; Ashraf, U.; Khan, I.; Wang, L. Alteration in growth, leaf gas exchange, and photosynthetic pigments of maize plants under combined cadmium and arsenic stress. *Water Air Soil Pollut.* **2017**, *228*, 13. [\[CrossRef\]](#)
8. Rady, M.M.; Hemida, K.A. Modulation of cadmium toxicity and enhancing cadmium-tolerance in wheat seedlings by exogenous application of polyamines. *Ecotoxicol. Environ. Saf.* **2015**, *119*, 178–185. [\[CrossRef\]](#)
9. Hasanuzzaman, M.; Hossain, M.A.; Fujita, M. Exogenous selenium pretreatment protects rapeseed seedlings from cadmium-induced oxidative stress by upregulating antioxidant defense and methylglyoxal detoxification systems. *Biol. Trace Elem. Res.* **2012**, *149*, 248–261. [\[CrossRef\]](#)
10. Anjum, S.A.; Tanveer, M.; Hussain, S.; Bao, M.; Wang, L.; Khan, I.; Shahzad, B. Cadmium toxicity in Maize (*Zea mays* L.): Consequences on antioxidant systems, reactive oxygen species and cadmium accumulation. *Environ. Sci. Pollut. Res.* **2015**, *22*, 17022–17030. [\[CrossRef\]](#)
11. Gratao, P.L.; Monteiro, C.C.; Tezotto, T.; Carvalho, R.F.; Alves, L.R.; Peters, L.P.; Azevedo, R.A. Cadmium stress antioxidant responses and root-to-shoot communication in grafted tomato plants. *Biomaterials* **2015**, *28*, 803–816. [\[CrossRef\]](#)
12. Shanying, H.E.; Xiaoe, Y.A.N.G.; Zhenli, H.E.; Baligar, V.C. Morphological and physiological responses of plants to cadmium toxicity: A review. *Pedosphere* **2017**, *27*, 421–438.
13. Xin, J.; Zhao, X.; Tan, Q.; Sun, X.; Hu, C. Comparison of cadmium absorption, translocation, subcellular distribution and chemical forms between two radish cultivars (*Raphanus sativus* L.). *Ecotoxicol. Environ. Saf.* **2017**, *145*, 258–265. [\[CrossRef\]](#) [\[PubMed\]](#)
14. Khan, F.; Hussain, S.; Tanveer, M.; Khan, S.; Hussain, H.A.; Iqbal, B.; Geng, M. Coordinated effects of lead toxicity and nutrient deprivation on growth, oxidative status, and elemental composition of primed and non-primed rice seedlings. *Environ. Sci. Pollut. Res.* **2018**, *25*, 21185–21194. [\[CrossRef\]](#) [\[PubMed\]](#)
15. Fahad, S.; Hussain, S.; Saud, S.; Tanveer, M.; Bajwa, A.A.; Hassan, S.; Shah, F. A biochar application protects rice pollen from high-temperature stress. *Plant Physiol. Biochem.* **2015**, *96*, 281–287. [\[CrossRef\]](#)
16. Liu, W.; Huo, R.; Xu, J.; Liang, S.; Li, J.; Zhao, T.; Wang, S. Effects of biochar on nitrogen transformation and heavy metals in sludge composting. *Bioresour. Technol.* **2017**, *235*, 43–49. [\[CrossRef\]](#)
17. Lu, K.; Yang, X.; Shen, J.; Robinson, B.; Huang, H.; Liu, D.; Wang, H. Effect of bamboo and rice straw biochars on the bioavailability of Cd, Cu, Pb and Zn to *Sedum plumbizincicola*. *Agric. Ecosyst. Environ.* **2014**, *191*, 124–132. [\[CrossRef\]](#)
18. Puga, A.P.; Abreu, C.A.; Melo, L.C.A.; Beesley, L. Biochar application to a contaminated soil reduces the availability and plant uptake of zinc, lead and cadmium. *J. Environ. Manag.* **2015**, *159*, 86–93. [\[CrossRef\]](#)
19. Zhang, Z.Y.; Jun, M.; Shu, D.; Chen, W.F. Effect of biochar on relieving cadmium stress and reducing accumulation in super japonica rice. *J. Integr. Agric.* **2014**, *13*, 547–553. [\[CrossRef\]](#)
20. Rehman, M.; Liu, L.; Bashir, S.; Saleem, M.H.; Chen, C.; Peng, D.; Siddique, K.H. Influence of rice straw biochar on growth, antioxidant capacity and copper uptake in ramie (*Boehmeria nivea* L.) grown as forage in aged copper-contaminated soil. *Plant Physiol. Biochem.* **2019**, *138*, 121–129. [\[CrossRef\]](#)
21. Joseph, S.; Anawar, H.M.; Storer, P.; Blackwell, P.; Chee, C.H.I.A.; Yun, L.I.N.; Solaiman, Z.M. Effects of enriched biochars containing magnetic iron nanoparticles on mycorrhizal colonisation, plant growth, nutrient uptake and soil quality improvement. *Pedosphere* **2015**, *25*, 749–760. [\[CrossRef\]](#)
22. Rizwan, M.; Noreen, S.; Ali, S.; Anwar, S.; ur Rehman, M.Z.; Qayyum, M.F.; Hussain, A. Influence of biochar amendment and foliar application of iron oxide nanoparticles on growth, photosynthesis, and cadmium accumulation in rice biomass. *J. Soils Sediments* **2019**, *19*, 3749–3759. [\[CrossRef\]](#)
23. O'Connor, D.; Peng, T.; Li, G.; Wang, S.; Duan, L.; Mulder, J.; Hou, D. Sulfur-modified rice husk biochar: A green method for the remediation of mercury contaminated soil. *Sci. Total Environ.* **2018**, *621*, 819–826. [\[CrossRef\]](#) [\[PubMed\]](#)
24. Wu, Q.; Xian, Y.; He, Z.; Zhang, Q.; Wu, J.; Yang, G.; Long, L. Adsorption characteristics of Pb (II) using biochar derived from spent mushroom substrate. *Sci. Rep.* **2019**, *9*, 1–11. [\[CrossRef\]](#) [\[PubMed\]](#)
25. Wang, Y.Y.; Ji, H.Y.; Lyu, H.H.; Liu, Y.X.; He, L.L.; You, L.C.; Yang, S.M. Simultaneous alleviation of Sb and Cd availability in contaminated soil and accumulation in *Lolium multiflorum* Lam. After amendment with Fe–Mn-Modified biochar. *J. Clean. Prod.* **2019**, *231*, 556–564. [\[CrossRef\]](#)

26. Mandal, S.; Sarkar, B.; Bolan, N.; Ok, Y.S.; Naidu, R. Enhancement of chromate reduction in soils by surface modified biochar. *J. Environ. Manag.* **2017**, *186*, 277–284. [\[CrossRef\]](#) [\[PubMed\]](#)
27. Lucena, J.J.; Hernandez-Apaolaza, L. Iron nutrition in plants: An overview. *Plant Soil* **2017**, *418*, 1–4. [\[CrossRef\]](#)
28. Jia, W.; Sun, X.; Gao, Y.; Yang, Y.; Yang, L. Fe-modified biochar enhances microbial nitrogen removal capability of constructed wetland. *Sci. Total Environ.* **2020**, *740*, 139534. [\[CrossRef\]](#)
29. Qiao, Y.; Wu, J.; Xu, Y.; Fang, Z.; Zheng, L.; Cheng, W.; Zhao, D. Remediation of cadmium in soil by biochar-supported iron phosphate nanoparticles. *Ecol. Eng.* **2017**, *106*, 515–522. [\[CrossRef\]](#)
30. Ahmad, M.; Ok, Y.S.; Rajapaksha, A.U.; Lim, J.E.; Kim, B.Y.; Ahn, J.H.; Lee, S.S. Lead and copper immobilization in a shooting range soil using soybean stover-and pine needle-derived biochars: Chemical, microbial and spectroscopic assessments. *J. Hazard. Mater.* **2016**, *301*, 179–186. [\[CrossRef\]](#)
31. Palansooriya, K.N.; Shaheen, S.M.; Chen, S.S.; Tsang, D.C.; Hashimoto, Y.; Hou, D.; Ok, Y.S. Soil amendments for immobilization of potentially toxic elements in contaminated soils: A critical review. *Environ. Int.* **2020**, *134*, 105046. [\[CrossRef\]](#)
32. Shen, Q.; Hedley, M.; Camps Arbestain, M.; Kirschbaum, M.U.F. Can biochar increase the bioavailability of phosphorus? *J. Soil Sci. Plant Nutr.* **2016**, *16*, 268–286. [\[CrossRef\]](#)
33. Shen, Z.; Tian, D.; Zhang, X.; Tang, L.; Su, M.; Zhang, L.; Hou, D. Mechanisms of biochar assisted immobilization of Pb²⁺ by bioapatite in aqueous solution. *Chemosphere* **2018**, *190*, 260–266. [\[CrossRef\]](#) [\[PubMed\]](#)
34. Igalavithana, A.D.; Lee, S.E.; Lee, Y.H.; Tsang, D.C.; Rinklebe, J.; Kwon, E.E.; Ok, Y.S. Heavy metal immobilization and microbial community abundance by vegetable waste and pine cone biochar of agricultural soils. *Chemosphere* **2017**, *174*, 593–603. [\[CrossRef\]](#) [\[PubMed\]](#)
35. O'Connor, D.; Peng, T.; Zhang, J.; Tsang, D.C.; Alessi, D.S.; Shen, Z.; Hou, D. Biochar application for the remediation of heavy metal polluted land: A review of in situ field trials. *Sci. Total Environ.* **2018**, *619*, 815–826. [\[CrossRef\]](#) [\[PubMed\]](#)
36. Matouq, M.; Jildeh, N.; Qtaishat, M.; Hindiyeh, M.; Al Syouf, M.Q. The adsorption kinetics and modeling for heavy metals removal from wastewater by Moringa pods. *J. Environ. Chem. Eng.* **2015**, *3*, 775–784. [\[CrossRef\]](#)
37. Saadi, R.; Saadi, Z.; Fazaeli, R.; Fard, N.E. Monolayer and multilayer adsorption isotherm models for sorption from aqueous media. *Korean J. Chem. Eng.* **2015**, *32*, 787–799. [\[CrossRef\]](#)
38. Ho, S.H.; Wang, D.; Wei, Z.S.; Chang, J.S.; Ren, N.Q. Lead removal by a magnetic biochar derived from persulfate-ZVI treated sludge together with one-pot pyrolysis. *Bioresour. Technol.* **2018**, *247*, 463–470.
39. Ayawei, N.; Ebelegi, A.N.; Wankasi, D. Modelling and interpretation of adsorption isotherms. *J. Chem.* **2017**. [\[CrossRef\]](#)
40. Liu, L.; Luo, X.B.; Ding, L.; Luo, S.L. Application of nanotechnology in the removal of heavy metal from water. In *Nanomaterials for the Removal of Pollutants and Resource Reutilization*; Elsevier: Amsterdam, The Netherlands, 2019; pp. 83–147.
41. Mustapha, A.A.; Abdu, N.; Jibrin, J.M. Adsorption of Cadmium, Copper, Lead and Zinc on Organically Amended Soil Fractions Using the Freundlich, Langmuir and Dubinin-Raduskevich Models. *Int. J. Soil Sci.* **2017**, *12*, 43–53. [\[CrossRef\]](#)
42. De Castro Alves, L.; Yáñez-Vilar, S.; Piñeiro-Redondo, Y.; Rivas, J. Novel Magnetic Nanostructured Beads for Cadmium (II) Removal. *Nanomaterials* **2019**, *9*, 356. [\[CrossRef\]](#)
43. Song, Z.; Lian, F.; Yu, Z.; Zhu, L.; Xing, B.; Qiu, W. Synthesis and characterization of a novel MnOx-loaded biochar and its adsorption properties for Cu²⁺ in aqueous solution. *Chem. Eng. J.* **2014**, *242*, 36–42. [\[CrossRef\]](#)
44. Tan, X.F.; Liu, Y.G.; Gu, Y.L.; Xu, Y.; Zeng, G.M.; Hu, X.J.; Li, J. Biochar-based nano-composites for the decontamination of wastewater: A review. *Bioresour. Technol.* **2016**, *212*, 318–333. [\[CrossRef\]](#) [\[PubMed\]](#)
45. Bradford, M.M. A rapid and sensitive method for the quantitation of microgram quantities of protein utilizing the principle of protein-dye binding. *Anal. Biochem.* **1976**, *72*, 248–254. [\[CrossRef\]](#)
46. Singleton, V.L.; Orthofer, R.; Lamuela-Raventós, R.M. [14] Analysis of total phenols and other oxidation substrates and antioxidants by means of folin-ciocalteu reagent. *Methods Enzymol.* **1999**, *299*, 152–178.
47. Strain, H.H.; SVEC, W.A. Extraction, separation, estimation, and isolation of the chlorophylls. In *The Chlorophylls*; Academic Press: Cambridge, MA, USA, 1966; pp. 21–66.
48. Jambunathan, N. Determination and detection of reactive oxygen species (ROS), lipid peroxidation, and electrolyte leakage in plants. In *Plant Stress Tolerance*; Humana Press: Totowa, NJ, USA, 2010; pp. 291–297.
49. Cakmak, I.; Marschner, H. Magnesium deficiency and high light intensity enhance activities of superoxide dismutase, ascorbate peroxidase, and glutathione reductase in bean leaves. *Plant Physiol.* **1992**, *98*, 1222–1227. [\[CrossRef\]](#)
50. Nakano, Y.; Asada, K. Hydrogen peroxide is scavenged by ascorbate-specific peroxidase in spinach chloroplasts. *Plant Cell Physiol.* **1981**, *22*, 867–880.
51. Jones, J.B. Plant tissue analysis in micronutrients. *Micronutr. Agric.* **1991**, *4*, 477–521.
52. Manzoor, Q.; Nadeem, R.; Iqbal, M.; Saeed, R.; Ansari, T.M. Organic acids pretreatment effect on *Rosa bourbonia* phyto-biomass for removal of Pb (II) and Cu (II) from aqueous media. *Bioresour. Technol.* **2013**, *132*, 446–452. [\[CrossRef\]](#)
53. Steel, R.G.D.; Torrie, J.H.; Dickey, D.A. Principles and procedures of statistics. In *A Bio-Metrical Approach*, 3rd ed.; McGraw Hill: New York, NY, USA, 1997.
54. Khan, W.D.; Ramzani, P.M.A.; Anjum, S.; Abbas, F.; Iqbal, M.; Yasar, A.; Ihsan, M.Z. Potential of miscanthus biochar to improve sandy soil health, in situ nickel immobilization in soil and nutritional quality of spinach. *Chemosphere* **2017**, *185*, 1144–1156. [\[CrossRef\]](#)

55. Tanveer, M.; Ahmed, H.A.I. ROS Signalling in Modulating Salinity Stress Tolerance in Plants. In *Salt and Drought Stress Tolerance in Plants*; Springer: Cham, Switzerland, 2020; pp. 299–314.
56. Tanveer, M.; Wang, L. Potential targets to reduce beryllium toxicity in plants: A review. *Plant Physiol. Biochem.* **2019**, *139*, 691–696. [[CrossRef](#)]
57. Hatata, M.M.; Abdel-Aal, E.A. Oxidative stress and antioxidant defense mechanisms in response to cadmium treatments. *J. Environ. Agric. Sci.* **2008**, *4*, 655–669.
58. Mishra, S.; Srivastava, S.; Tripathi, R.D.; Govindarajan, R.; Kuriakose, S.V.; Prasad, M.N.V. Phytochelatin synthesis and response of antioxidants during cadmium stress in *Bacopa monnieri* L. *Plant Physiol. Biochem.* **2006**, *44*, 25–37. [[CrossRef](#)] [[PubMed](#)]
59. Mehdizadeh, L.; Moghaddam, M.; Lakzian, A. Response of summer savory at two different growth stages to biochar amendment under NaCl stress. *Arch. Agron. Soil Sci.* **2019**, *65*, 1120–1133. [[CrossRef](#)]
60. Tanveer, M.; Shabala, S. Targeting redox regulatory mechanisms for salinity stress tolerance in crops. In *Salinity Responses and Tolerance in Plants*; Springer: Cham, Switzerland, 2018; Volume 1, pp. 213–234.
61. Mohamed, A.A.; Aly, A.A. Iron deficiency stimulated some enzymes activity, lipid peroxidation and free radicals production in *Borage officinalis* induced in vitro. *Int. J. Agric. Biol.* **2004**, *6*, 179–184.
62. Fourcroy, P.; Vansuyt, G.; Kushnir, S.; Inzé, D.; Briat, J.F. Iron-regulated expression of a cytosolic ascorbate peroxidase encoded by the APX1 gene in Arabidopsis seedlings. *Plant Physiol.* **2004**, *134*, 605–613. [[CrossRef](#)] [[PubMed](#)]
63. Mozafari, A.A.; Ghaderi, N. Grape response to salinity stress and role of iron nanoparticle and potassium silicate to mitigate salt induced damage under in vitro conditions. *Physiol. Mol. Biol. Plants* **2018**, *24*, 25–35. [[CrossRef](#)] [[PubMed](#)]
64. Ivanov, A.A.; Kosobryukhov, A.A. Ecophysiology of Plants under Cadmium Toxicity: Photosynthetic and Physiological Responses. In *Plant Ecophysiology and Adaptation under Climate Change: Mechanisms and Perspectives I*; Springer: Singapore, 2020; pp. 429–484.
65. Su, Y.; Qin, C.; Begum, N.; Ashraf, M.; Zhang, L. Acetylcholine ameliorates the adverse effects of cadmium stress through mediating growth, photosynthetic activity and subcellular distribution of cadmium in tobacco (*Nicotiana benthamiana* L.). *Ecotoxicol. Environ. Saf.* **2020**, *198*, 110671. [[CrossRef](#)]
66. Liu, H.; Yang, L.; Li, N.; Zhou, C.; Feng, H.; Yang, J.; Han, X. Cadmium toxicity reduction in rice (*Oryza sativa* L.) through iron addition during primary reaction of photosynthesis. *Ecotoxicol. Environ. Saf.* **2020**, *200*, 110746. [[CrossRef](#)]
67. Xu, C.Y.; Hosseini-Bai, S.; Hao, Y.; Rachaputi, R.C.; Wang, H.; Xu, Z.; Wallace, H. Effect of biochar amendment on yield and photosynthesis of peanut on two types of soils. *Environ. Sci. Pollut. Res.* **2015**, *22*, 6112–6125. [[CrossRef](#)]
68. Younis, U.; Malik, S.A.; Rizwan, M.; Qayyum, M.F.; Ok, Y.S.; Shah, M.H.R.; Ahmad, N. Biochar enhances the cadmium tolerance in spinach (*Spinacia oleracea*) through modification of Cd uptake and physiological and biochemical attributes. *Environ. Sci. Pollut. Res.* **2016**, *23*, 21385–21394. [[CrossRef](#)]
69. Keshavarz Afshar, R.; Hashemi, M.; DaCosta, M.; Spargo, J.; Sadeghpour, A. Biochar application and drought stress effects on physiological characteristics of *Silybum marianum*. *Commun. Soil Sci. Plant Anal.* **2016**, *47*, 743–752. [[CrossRef](#)]
70. Parmar, P.; Kumari, N.; Sharma, V. Structural and functional alterations in photosynthetic apparatus of plants under cadmium stress. *Bot. Sci.* **2013**, *54*, 45. [[CrossRef](#)] [[PubMed](#)]
71. Bashir, K.; Rasheed, S.; Kobayashi, T.; Seki, M.; Nishizawa, N.K. Regulating subcellular metal homeostasis: The key to crop improvement. *Front. Plant Sci.* **2016**, *7*, 1192. [[CrossRef](#)]
72. Anjum, S.A.; Tanveer, M.; Hussain, S.; Shahzad, B.; Ashraf, U.; Fahad, S.; Bajwa, A.A. Osmoregulation and antioxidant production in maize under combined cadmium and arsenic stress. *Environ. Sci. Pollut. Res.* **2016**, *23*, 11864–11875. [[CrossRef](#)] [[PubMed](#)]
73. Anjum, S.A.; Tanveer, M.; Hussain, S.; Ullah, E.; Wang, L.; Khan, I.; Shahzad, B. Morpho-physiological growth and yield responses of two contrasting maize cultivars to cadmium exposure. *Clean (Weinh)* **2016**, *44*, 29–36. [[CrossRef](#)]
74. Grato, P.L.; Monteiro, C.C.; Rossi, M.L.; Martinelli, A.P.; Peres, L.E.; Medici, L.O.; Azevedo, R.A. Differential ultrastructural changes in tomato hormonal mutants exposed to cadmium. *Environ. Exp. Bot.* **2009**, *67*, 387–394. [[CrossRef](#)]
75. Farhangi-Abriz, S.; Torabian, S. Antioxidant enzyme and osmotic adjustment changes in bean seedlings as affected by biochar under salt stress. *Ecotoxicol. Environ. Saf.* **2017**, *137*, 64–70. [[CrossRef](#)]
76. Gupta, D.K.; Pena, L.B.; Romero-Puertas, M.C.; Hernández, A.; Inouhe, M.; Sandalio, L.M. NADPH oxidases differentially regulate ROS metabolism and nutrient uptake under cadmium toxicity. *Plant Cell Environ.* **2017**, *40*, 509–526. [[CrossRef](#)]
77. Lehmann, J.; Joseph, S. *Biochar for Environmental Management: Science, Technology and Implementation*; Routledge: Abingdon, UK, 2015.
78. Kizito, S.; Luo, H.; Lu, J.; Bah, H.; Dong, R.; Wu, S. Role of nutrient-enriched biochar as a soil amendment during maize growth: Exploring practical alternatives to recycle agricultural residuals and to reduce chemical fertilizer demand. *Sustainability* **2019**, *11*, 3211. [[CrossRef](#)]
79. Xu, G.; Lv, Y.; Sun, J.; Shao, H.; Wei, L. Recent advances in biochar applications in agricultural soils: Benefits and environmental implications. *Clean (Weinh)* **2012**, *40*, 1093–1098. [[CrossRef](#)]
80. Biederman, L.A.; Harpole, W.S. Biochar and its effects on plant productivity and nutrient cycling: A meta-analysis. *GCB Bioenergy* **2013**, *5*, 202–214. [[CrossRef](#)]
81. Song, Y.; Jin, L.; Wang, X. Cadmium absorption and transportation pathways in plants. *Int. J. Phytoremediat.* **2017**, *19*, 133–141. [[CrossRef](#)] [[PubMed](#)]
82. Uruguchi, S.; Kamiya, T.; Sakamoto, T.; Kasai, K.; Sato, Y.; Nagamura, Y.; Fujiwara, T. Low-affinity cation transporter (OsLCT1) regulates cadmium transport into rice grains. *Proc. Natl. Acad. Sci. USA* **2011**, *108*, 20959–20964. [[CrossRef](#)] [[PubMed](#)]

83. Bari, M.A.; Akther, M.S.; Reza, M.A.; Kabir, A.H. Cadmium tolerance is associated with the root-driven coordination of cadmium sequestration, iron regulation, and ROS scavenging in rice. *Plant Physiol. Biochem.* **2019**, *136*, 22–33. [\[CrossRef\]](#)
84. Ma, X.; Liu, H.; Cao, H.; Qi, R.; Yang, K.; Zhao, R.; Zhang, Y. Genome-wide analysis of zinc-and iron-regulated transporter-like protein family members in apple and functional validation of ZIP10. *Biometals* **2019**, *32*, 657–669. [\[CrossRef\]](#)
85. Yu, R.; Ma, Y.; Li, Y.; Li, X.; Liu, C.; Du, X.; Shi, G. Comparative transcriptome analysis revealed key factors for differential cadmium transport and retention in roots of two contrasting peanut cultivars. *BMC Genom.* **2018**, *19*, 938. [\[CrossRef\]](#) [\[PubMed\]](#)
86. Bashir, K.; Ishimaru, Y.; Nishizawa, N.K. Iron uptake and loading into rice grains. *Rice* **2010**, *3*, 122–130. [\[CrossRef\]](#)
87. Ishimaru, Y.; Takahashi, R.; Bashir, K.; Shimo, H.; Senoura, T.; Sugimoto, K.; Nakanishi, H. Characterizing the role of rice NRAMP5 in manganese, iron and cadmium transport. *Sci. Rep.* **2012**, *2*, 286. [\[CrossRef\]](#) [\[PubMed\]](#)
88. Satoh-Nagasawa, N.; Mori, M.; Nakazawa, N.; Kawamoto, T.; Nagato, Y.; Sakurai, K.; Akagi, H. Mutations in rice (*Oryza sativa*) heavy metal ATPase 2 (OsHMA2) restrict the translocation of zinc and cadmium. *Plant Cell Physiol.* **2012**, *53*, 213–224. [\[CrossRef\]](#)
89. Miyadate, H.; Adachi, S.; Hiraizumi, A.; Tezuka, K.; Nakazawa, N.; Kawamoto, T.; Satoh-Nagasawa, N. OsHMA3, a P1B-type of ATPase affects root-to-shoot cadmium translocation in rice by mediating efflux into vacuoles. *New Phytol.* **2011**, *189*, 190–199. [\[CrossRef\]](#)
90. Thomine, S.; Wang, R.; Ward, J.M.; Crawford, N.M.; Schroeder, J.I. Cadmium and iron transport by members of a plant metal transporter family in Arabidopsis with homology to Nramp genes. *Proc. Natl. Acad. Sci. USA* **2000**, *97*, 4991–4996. [\[CrossRef\]](#)
91. Nazar, R.; Iqbal, N.; Masood, A.; Khan, M.I.R.; Syeed, S.; Khan, N.A. Cadmium toxicity in plants and role of mineral nutrients in its alleviation. *Am. J. Plant Sci.* **2012**, *3*, 1476–1489. [\[CrossRef\]](#)
92. Clemens, S.; Deinlein, U.; Ahmadi, H.; Höreth, S.; Uruguchi, S. Nicotianamine is a major player in plant Zn homeostasis. *Biometals* **2013**, *26*, 623–632. [\[CrossRef\]](#) [\[PubMed\]](#)
93. Guerinot, M.L. The ZIP family of metal transporters. *Biochim. Biophys. Acta. Biomembr.* **2000**, *1465*, 190–198. [\[CrossRef\]](#)
94. Ismael, M.; Elyamine, A.; Zhao, Y.; Moussa, M.; Rana, M.; Afzal, J.; Hu, C. Can selenium and molybdenum restrain cadmium toxicity to pollen grains in *Brassica napus*? *Int. J. Mol. Sci.* **2018**, *19*, 2163. [\[CrossRef\]](#)
95. Tran, T.A.; Popova, L.P. Functions and toxicity of cadmium in plants: Recent advances and future prospects. *Turk. J. Bot.* **2013**, *37*, 1–13.
96. Leupin, O.X.; Hug, S.J. Oxidation and removal of arsenic (III) from aerated groundwater by filtration through sand and zero-valent iron. *Water Res.* **2005**, *39*, 1729–1740. [\[CrossRef\]](#)
97. Ming, L.; Naimei, Y.; Huayong, H. Remediation of available Cd and Pb contamination in acidic soil by ferric chloride and ferric sulfate. *Chin. J. Environ. Eng.* **2015**, *9*, 469–476.
98. Wu, C.; Shi, L.; Xue, S.; Li, W.; Jiang, X.; Rajendran, M.; Qian, Z. Effect of sulfur-iron modified biochar on the available cadmium and bacterial community structure in contaminated soils. *Sci. Total Environ.* **2019**, *647*, 1158–1168. [\[CrossRef\]](#)
99. Lyu, H.; Tang, J.; Cui, M.; Gao, B.; Shen, B. Biochar/iron (BC/Fe) composites for soil and groundwater remediation: Synthesis, applications, and mechanisms. *Chemosphere* **2020**, *246*, 125609. [\[CrossRef\]](#)
100. Iqbal, M.J.; Farhan, C.; Khalil, A.; Munawar, I.; Mushtaq, M.; Naeem, M.A.; Bokhari, T.H. Kinetic study of Cr (III) and Cr (VI) biosorption using *Rosa damascena* phytomass: A rose waste biomass. *Asian J. Chem.* **2013**, *25*, 2099–2103. [\[CrossRef\]](#)
101. Cope, C.O.; Webster, D.S.; Sabatini, D.A. Arsenate adsorption onto iron oxide amended rice husk char. *Sci. Total Environ.* **2014**, *488*, 554–561. [\[CrossRef\]](#)
102. He, R.; Peng, Z.; Lyu, H.; Huang, H.; Nan, Q.; Tang, J. Synthesis and characterization of an iron-impregnated biochar for aqueous arsenic removal. *Sci. Total Environ.* **2018**, *612*, 1177–1186. [\[CrossRef\]](#)
103. Samsuri, A.W.; Sadegh-Zadeh, F.; Seh-Bardan, B.J. Adsorption of As (III) and As (V) by Fe coated biochars and biochars produced from empty fruit bunch and rice husk. *J. Environ. Chem. Eng.* **2013**, *1*, 981–988. [\[CrossRef\]](#)
104. Lefèvre, E.; Bossa, N.; Gardner, C.M.; Gehrke, G.E.; Cooper, E.M.; Stapleton, H.M.; Gunsch, C.K. Biochar and activated carbon act as promising amendments for promoting the microbial debromination of tetrabromobisphenol A. *Water Res.* **2018**, *128*, 102–110. [\[CrossRef\]](#) [\[PubMed\]](#)
105. Wang, S.; Gao, B.; Li, Y.; Creamer, A.E.; He, F. Adsorptive removal of arsenate from aqueous solutions by biochar supported zero-valent iron nanocomposite: Batch and continuous flow tests. *J. Hazard. Mater* **2017**, *322*, 172–181. [\[CrossRef\]](#) [\[PubMed\]](#)
106. Wei, D.; Li, B.; Huang, H.; Luo, L.; Zhang, J.; Yang, Y.; Zhou, Y. Biochar-based functional materials in the purification of agricultural wastewater: Fabrication, application and future research needs. *Chemosphere* **2018**, *197*, 165–180. [\[CrossRef\]](#) [\[PubMed\]](#)
107. Yao, Y.; Zhang, Y.; Gao, B.; Chen, R.; Wu, F. Removal of sulfamethoxazole (SMX) and sulfapyridine (SPY) from aqueous solutions by biochars derived from anaerobically digested bagasse. *Environ. Sci. Pollut. Res.* **2018**, *25*, 25659–25667. [\[CrossRef\]](#) [\[PubMed\]](#)